Available online at www.sciencedirect.com

ScienceDirect

Procedia Computer Science 221 (2023) 549–556

Procedia Computer Science

www.elsevier.com/locate/procedia

Information Technology and Quantitative Management (ITQM 2023)

# Infrared Small-Target Detection Based on Multi-level Local Contrast Measure

Haotian Sun[a], Qiuyu Jin[a], Jun Xu[a], Linbo Tang[a,*]

[a]*School of Information and Electronics,Beijing University of Technology, Beijing 100081, China*

## Abstract

Infrared small target detection technology is one of the key technologies for reconnaissance, guidance, and early warning systems, and it has important theoretical and practical value to conduct in-depth research on it. However, there are several challenges in infrared small target detection. Firstly, infrared small targets have low signal-to-noise ratio, which makes them easily submerged in complex backgrounds. Secondly, since infrared small target detection is a long-distance imaging process, there is no shape or texture information available, which increases the difficulty of target detection. To address these challenges, this paper proposes a multi-level contrast enhancement method to suppress structural background, and develops a more effective detection algorithm. Based on the concept of local contrast measurement (LCM), a new contrast-based small target detection algorithm called Multi-Level Local Contrast Measurement (MLLCM) is constructed, and its effective implementation process is provided. Compared with LCM, MPCM(Multiscale Patch-based Contrast Measure), and other algorithms, this algorithm effectively enhances the target area and eliminates background clutter. The results on simulated images demonstrate the effectiveness of this algorithm.



*Keywords:* Infrared target ; Mlti-level contrast ; Contrast measurement ; Detection ;

## 1. Introduction

Some common forms of image representation are optical images, infrared images, and synthetic aperture radar (SAR) images. Optical images have high resolution and reflect the contour of the target. Infrared images reflect the thermal radiation characteristics of the target, while SAR images can reflect the electromagnetic radiation characteristics of the target. Therefore, using these different properties, a series of applications such as object detection, tracking, and segmentation can be performed [1, 2, 3, 4, 5, 6].Infrared imaging has several advantages, including strong anti-interference ability, strong concealment, and passive detection capabilities.The detection of infrared small targets plays a crucial role in the study of infrared imaging systems and is widely used in warning and target tracking tasks. However, the presence of cloud clutter or sea clutter often submerges small targets in complex backgrounds, resulting in low signal-to-noise ratio. Moreover, small targets lack specific textures or shapes due to the long imaging distance. Therefore, the detection of infrared small targets is widely regarded as a challenging and difficult task.

*Corresponding author: Linbo Tang.
*E-mail address:* tanglinbo@bit.edu.cn.


10.1016/j.procs.2023.08.021

Infrared small target detection algorithms are categorized based on their utilization of inter-frame correlation information; these include weak small target detection based on infrared sequences and weak small target detection based on single-frame infrared images. Since weak small target detection based on infrared sequences is limited by the computer's computational capabilities and involves single-frame detection methods in the process, the detection efficiency of single-frame detection directly affects the time complexity and detection rate of multi-frame detection algorithms. Therefore, the weak small target detection based on single-frame infrared images has been the primary focus of research in recent years.

Weak small target detection methods based on single-frame infrared images include filtering-based methods [7, 8] , methods based on the human visual system, and methods based on low-rank and sparse recovery [9, 10]. In practical applications, humans can easily distinguish infrared small targets from complex backgrounds, mainly due to the selective attention mechanism of the human visual system [11]. Methods for detecting small targets based on the human visual system have been one of the hot research topics in recent years. Chen et al. [12] proposed a Local Contrast Measure (LCM) method, which quantitatively calculates the gray differences between the center block and neighboring blocks, and takes the maximum value at multiple scales. LCM has a strong ability to enhance the target area. However, LCM amplifies the salt noise of a single pixel, which increases the number of false alarms. Wei et al. [13] proposed a Multiscale Patch-based Contrast Measure (MPCM) method for detecting infrared small targets based on multiscale blocks. In the Patch-based Contrast Measure (PCM) based on multiscale patches, each region of interest is divided into 9 patches, and the dissimilarity between the surrounding patches and the central patch is calculated. The directional differences are multiplied, and the result is selected minimally to obtain the final output. However, this method does not fully utilize the characteristic of small target energy distribution that approximates a Gaussian distribution [14]. It cannot effectively eliminate high-brightness false targets and introduces many false alarms in complex backgrounds. Saed Moradi et al. [15] proposed an Absolute Directional Mean Difference (ADMD) algorithm-based rapid and robust detection method for infrared small targets. This method uses the directional information of the center block and surrounding neighborhood blocks to characterize the contrast of the Region of Interest (ROI). However, this method may mistakenly detect high-brightness small objects as small targets in complex backgrounds, such as forests and ground conditions, leading to unnecessary false alarms.

In summary, there are two main issues with existing methods. Firstly, most methods are based on the contrast between the target and background, but infrared images are often characterized by low detail and high noise, making it difficult to distinguish small targets from the background. Additionally, most existing methods assume that the target has a high signal-to-noise ratio and are mainly used to detect bright targets in darker surroundings, but there may be both bright and weak small targets in an image, and weak small targets are easily interfered with by the background and bright targets. When using the same structural window to calculate the target's contrast, weak small targets with low grayscale values have lower contrast and are susceptible to false alarms.

Therefore, this article proposes a locally graded contrast measurement method that uses different structural windows to measure the local contrast of targets in different grayscale ranges. A single-layer local contrast measurement method is used to calculate the local contrast of targets with high grayscale values, while a double-layer local contrast measurement method is used to increase contrast and reduce the impact of bright targets and the background on weak small targets with low grayscale values. This method considers the energy distribution characteristics of the target while highlighting small targets and can be used in complex scenes with non-uniform backgrounds.

## 2. Related work

### *2.1. Patch-based Contrast Measure*

The sliding window consists of 9 sub-blocks, each of which is the same size and ideally should be equal to the size of the small target (as shown in Figure 1.(*a*)).

If the window size is smaller than the size of the small target, it may mistakenly detect the small target as background. If the window size is too large, computational complexity will increase.Considering that the size of targets is generally within $5 \times 5$ pixels [16]. A multi-scale method is employed, with sub-blocks set to $3 \times 3$ and $5 \times 5$. The two scales of sliding windows are used to calculate the target's contrast by sliding from top to bottom, left to right on the image.

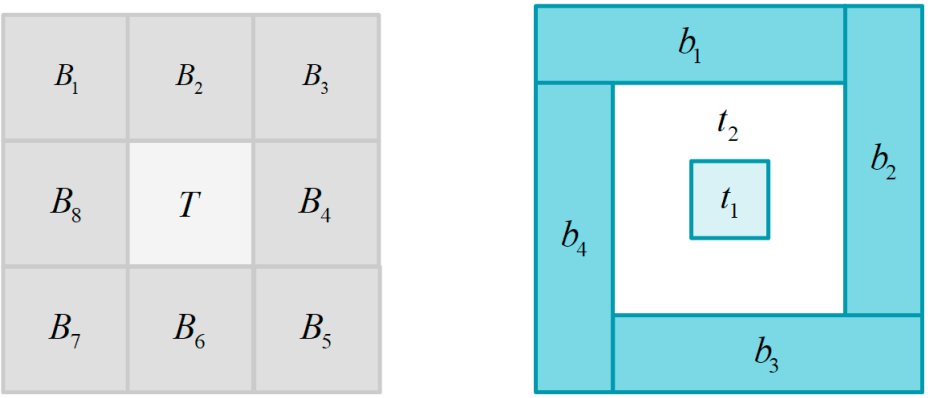


Fig. 1. (a) Structure window of PCM; (b) Structure window of proposed algorithm.

For Figure 1.($a$), the response value of each sub-block is represented by its mean value,

$$m_{Bi} = \frac{1}{k}\sum_{j=1}^{k} I_j^{(i)} \tag{1}$$

In the formula: $m_{Bi}$ is the response value of the sub block, $k$ is the number of pixels in the sub block, and $I_j^{(i)}$ is the pixel value of the jth pixel in the i-th sub block.

Similarly, the response value of the center sub-block $T$ is:

$$T = \frac{1}{k}\sum_{j=1}^{k} I_j \tag{2}$$

In the formula, $T$ is the response value of the central sub block, $k$ is the number of pixels in the sub block, and $I_j$ is the pixel value of the jth pixel in the $T$ sub block.

There is discontinuity in the spatial distribution between small targets and the background, and detecting small targets requires characterizing the discontinuity between the two. Use $d(T, B_i)$ to represent the difference between the central sub block and the neighboring sub block.

$$d(T, B_i) = m_T - m_{B_i}, \quad i = 1, \ldots, 8 \tag{3}$$

By using $d(T, B_i)$ , local contrast measures can be given at a certain scale.To characterize this property, we define it as:

$$\tilde{d}_i = d(T, B_i) \times d(T, B_{i+4}), \quad i = 1, \ldots, 4 \tag{4}$$

$\tilde{d}_i$ measures the similarity between the central and background sub blocks in the i-th direction. When $\tilde{d}_i > 0$ , it indicates that the signs of $d(T, B_i)$ and $d(T, B_{i+4})$ are the same, indicating that the bright or dark target is at the center of the sliding window.

In small target enhancement, the contrast between the target area and the background area should be as large as possible. Therefore, the minimum distance between the central sub-block and its surrounding background sub-blocks can be used as a measure of comparison. Therefore, we can calculate the PCM at a given scale as follows:

$$c_{x,y} = \min \tilde{d}_i (i = 1, \ldots, 4) \tag{5}$$

In the above equation, $x, y$ represents the coordinate of any point in the image. By taking the minimum contrast among the four directions of the sliding window, $c_{x,y}$ can be obtained.

## 3. Proposed work

### 3.1. Overall workflow

My work mainly consists of three steps: image pre-processing, multi-level contrast enhancement, and threshold segmentation. Firstly, We perform image pre-processing by applying mean filtering to the infrared original image using a specific window structure to suppress background noise. Secondly, We use multi-level contrast enhancement to expand the differences between the target and background areas, thus enhancing the signal-to-noise ratio of the target. Lastly, We conduct threshold segmentation to extract target features.

### 3.2. Pre-processing

The purpose of preprocessing is to prepare for subsequent image detection and eliminate noise.Introducing a new sliding window that consists of 6 sub-blocks arranged in 3 layers. The innermost layer contains the smallest sub-block, while the middle layer sub-blocks have an area 8 times that of the innermost layer. The four sub-blocks of the outermost layer have equal area, which is 4 times that of the innermost layer (as shown in figure 1.(*b*)).

Considering that the size of bright targets is generally within $5 \times 5$ pixels and the size of weak small targets is within $3 \times 3$ pixels, this paper uses two different structural windows to calculate bright targets and weak small targets based on their grayscale ranges.For bright targets, a window as shown in Figure 1.(*a*) is used. For weak small targets, a window as shown in Figure 1.(*b*) is used. Sub-blocks are set to 1, and a sliding window is used to calculate contrast by sliding from top to bottom, left to right on the image.

For Figure 1.(*b*), the response value of each sub-block is represented by its mean value,

$$m_{bi} = \frac{1}{k} \sum_{j=1}^{k} I_j^{(i)} \tag{6}$$

In the formula: $m_{bi}$ is the response value of the sub block, $k$ is the number of pixels in the sub block, and $I_j^{(i)}$ is the pixel value of the jth pixel in the i-th sub block.

Similarly, the response value of the center sub-block $t_1$ ,$t_2$ is:

$$\begin{aligned} t_1 &= \tfrac{1}{k} \textstyle\sum_{j=1}^{k} I_j \\ t_2 &= \tfrac{1}{k} \textstyle\sum_{j=1}^{k} I_j \end{aligned} \tag{7}$$

In the formula, $t_1$ represents the response value of the central sub-block in the innermost layer, $t_2$ represents the response value of the central sub-block in the middle layer, $k$ represents the number of pixels in the sub-block, and $I_j$ represents the pixel value of the i-th pixel in the $T$ sub-block.

Using the mean value to represent the response value can eliminate the influence of single-pixel noise, achieving the effect of filtering.

### 3.3. Double layer contrast enhancement

The detection of dim targets can be challenging due to their small area and low contrast with the background. Traditional MPCM characterization may miss these targets. To overcome this issue, a window structure (shown in Figure 1.(*b*)) is proposed to measure the local contrast of dim targets.The spatial distribution of small targets, target radiation, and background radiation is discontinuous, which makes it necessary to characterize the discontinuity between the three in order to detect small targets.The difference between the center sub-block $t_1$ and the middle sub-block $t_2$ is represented by $d(t_1, t_2)$, which serves as an indicator of the local contrast between the target and target radiation. The difference between the middle sub-block $t_2$ and the outermost sub-block $b_j$ is represented by $d(t_2, b_j)$, which serves as an indicator of the local contrast between the target radiation and background.

$$\begin{aligned} d\left(t_1, t_2\right) &= m_{t_1} - m_{t_2} \\ d\left(t_2, b_j\right) &= m_{t_2} - m_{b_j}, \quad j = 1, \ldots, 4 \end{aligned} \tag{8}$$

By using $d\left(t_2, b_j\right)$ , local contrast measures can be given at a certain scale.To characterize this property, we define it as:

$$\tilde{d}_j = d\left(t_2, b_j\right) \times d\left(t_2, b_{j+2}\right), \quad j = 1, \ldots, 2 \tag{9}$$

$\tilde{d}_j$ measures the similarity between the central and background sub blocks in the j-th direction. When $\tilde{d}_j > 0$, it indicates that the signs of $d\left(t_2, b_j\right)$ and $d\left(t_2, b_{j+2}\right)$ are the same, indicating that the bright or dark target is at the center of the sliding window. Due to the fact that in general, the small targets that need to be detected are all bright targets. So this article takes the case where the two terms on the right side of the expression $\tilde{d}_j$ are both positive numbers, that is, detecting bright targets.

$$\tilde{D}_j = \tilde{d}j \times H\left[d\left(t_2, b_j\right)\right] \times H\left[d\left(t_2, b_{j+2}\right)\right] (j = 1, \ldots, 2) \tag{10}$$

In the above formula,$\tilde{D}_j$ represents the dissimilarity between the center sub-block and the background sub-block in the $i$-th direction, assuming that the target is a bright object.$H(\bullet)$ is the Heaviside step function, defined as follows:

$$H(t) = \begin{cases} 1, & t \geq 0 \\ 0, & t < 0 \end{cases} \tag{11}$$

In small object enhancement, maximizing the contrast between the target area and the background area is essential. Therefore, the minimum distance between the central sub-block and the surrounding background sub-blocks can serve as a measure of contrast. Accordingly, we can calculate the dual-contrast measure value for a given dimension in the following way.

$$\hat{e}_{x,y} = \min d\left(t_1, t_2\right) \times \tilde{D}_j (j = 1, \ldots, 2) \tag{12}$$

The equation above represents this process, where (x, y) denotes the coordinates of any point in the image. The minimum contrast between the two directions of the sliding window results in $\hat{e}_{x,y}$.

Considering the better measurement effect of MPCM on bright targets, dual-contrast enhancement has a better effect on detecting dark and weak targets. To further improve target detection, some modifications were made to MPCM to only detect bright targets. Therefore, we can calculate the PCM for a given dimension in the following way.

$$c'_{x,y} = \min \tilde{d}_i \times H\left[d\left(T, B_i\right)\right] \times H\left[d\left(T, B_{i+4}\right)\right] (i = 1, \ldots, 4) \tag{13}$$

Taking into account the size of the target, we calculate the PCM saliency map at two scales, 3×3 and 5×5, and then take the maximum value of the results at each pixel point to obtain the MPCM saliency map. The specific process is shown in the following equation.

$$\hat{c}_{x,y} = \max\left\{c'^{(1)}_{x,y}, c'^{(2)}_{x,y}\right\} \tag{14}$$

In the above equation, $\hat{c}_{x,y}$ represents the pixel value of the point with coordinates $x, y$ in the MPCM saliency image, while $c'^{(1)}_{x,y}$ and $c'^{(2)}_{x,y}$ represent the pixel values of the $x, y$ point at scales 3×3 and 5×5, respectively. MPCM is effective in suppressing the background and enhancing the target by quantitatively characterizing the dissimilarity between the target and the background within the neighborhood. However, there are certain limitations to the MPCM method.

In an image, there may be both bright and dark targets, and the contrast measurement methods used depend on the grayscale range.

$$E(x, y) = \begin{cases} \hat{c}_{x,y}, & I_{x,y} > \alpha \\ \hat{e}_{x,y}, & I_{x,y} \leq \alpha \end{cases} \tag{15}$$

In the equation above, $x, y$ represents the coordinates of any point in the image, and $I_{x,y}$ is the grayscale value of the point.$\alpha$ denotes the grayscale threshold, where multi-scale contrast measurement is used for grayscale values greater than $\alpha$, and double-layer contrast enhancement is used for grayscale values less than or equal to $\alpha$.

### 3.4. Target extraction

Sliding window E calculation from top to bottom and left to right can yield a saliency map, which can then be used for object segmentation through an adaptive thresholding method.

$$\tau = \mu + k\sigma. \tag{16}$$

In the equation mentioned earlier,$\tau$ represents the threshold, and if the pixel value in the saliency image is greater than $\tau$ , it is set to 1; otherwise, it is set to 0, thus generating a binary image. $\mu$ denotes the mean of the saliency image, $k$ is the segmentation coefficient, usually ranging between $7 - 12$ , and $\sigma$ represents the standard deviation of the saliency image.

## 4. Experimental results and analysis

### 4.1. Data sources

The experimental data mainly consists of simulated data based on ground and sky backgrounds, as well as infrared images captured by unmanned aerial vehicles (UAVs). Figure 2 displays four infrared images taken in different scenarios. Figure 2.($a$) shows an infrared image with a building in the background, Figure 2.($b$) shows an infrared image with the ground as the background, Figure 2.($c$) shows an infrared image with clouds as the background, and Figure 2.($d$) shows an infrared Image of Sky Background from Satellite Perspective.

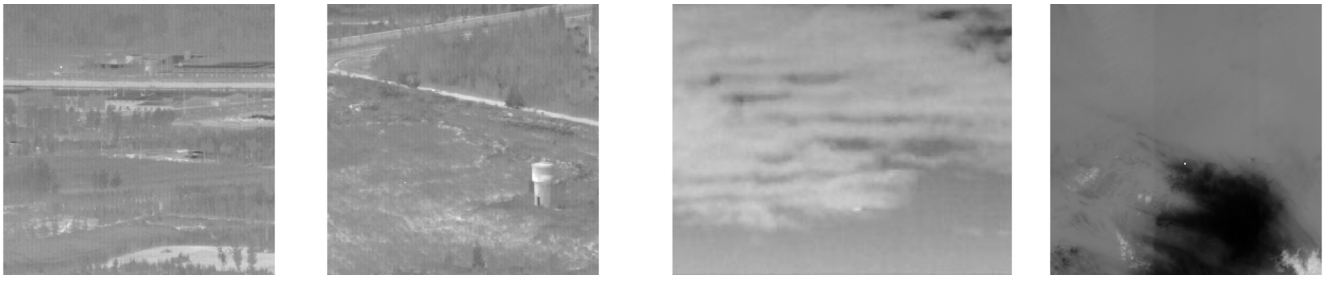

(a) (b) (c) (d)

Fig. 2. Infrared raw image.

### 4.2. Description of evaluation indicators

The evaluation criteria for the experiment mainly consider the detection rate $P_d$ and false alarm rate $P_f$.

$$P_d = \frac{N_d}{N_g}. \tag{17}$$

$$P_f = \frac{N_f}{N_t}. \tag{18}$$

In the equations, $N_d$ and $N_g$ represent the number of detected targets and the actual number of true targets, respectively. $N_f$ represents the number of false alarm targets, while $N_t$ represents the total number of detected targets. In equation (17), $P_d$ represents the detection rate, which is defined as the ratio of the number of correctly detected small targets in the image to the actual number of small targets . In equation (18), $P_f$ represents the false alarm rate, which is defined as the ratio of the number of small targets detected incorrectly in the image to the total number of small targets detected. To be considered correctly detected, a small target in the image must satisfy two conditions:

- the detection result overlaps with the real target in the image;
- the difference between the center pixel position of the detection result and the center pixel position of the real target does not exceed a certain range, usually within 5 pixels.

### 4.3. Qualitative analysis

The article proposes a method that improves the MPCM method in order to enhance the signal-to-noise ratio of small target images. To better illustrate this improvement, a 3D response map of the processed image is provided. Figures 3.(*a*) – (*d*) illustrate the original grayscale images, original grayscale response images, grayscale response images processed by the MPCM algorithm, grayscale response images processed by the proposed algorithm, and the detection results of the proposed algorithm, respectively. The 3D image indicates that the proposed method is effective in enhancing the signal-to-noise ratio of small target images.

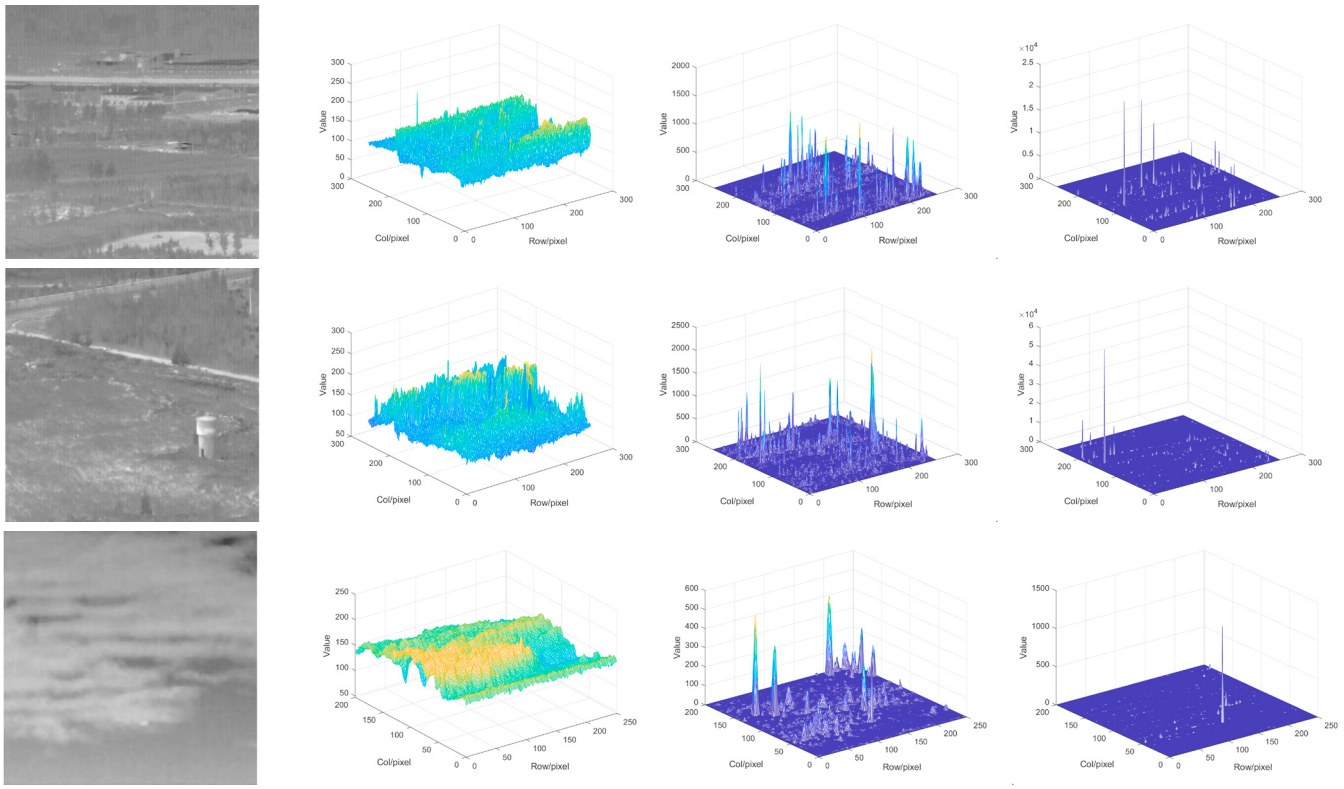


Fig. 3. Experimental results of response maps. (a)Original infrared image; (b)Original gray maps; (c)Gray response maps using MPCM alogrithm; (d)Gray response maps using

### 4.4. Quantitative analysis

In order to more intuitively demonstrate the performance of the algorithm, in the experiment, the first 20 frames of image sequences from three different scenes (cloud background, forest and building background, and ground background) were selected to calculate their detection rate and false alarm rate. The comparison was made with LCM, MPCM, and LMWIE algorithms.

Since both the proposed algorithm and the reference algorithms achieved a detection rate of around 100%, only the false alarm rate was compared. Table 1 below shows the false alarm rate data for the three different scenes.

From Table 1, it can be observed that the false alarm rate of the proposed algorithm is lower than that of the LMWIE algorithm by 1.93% in the ground background scene, and it is 0 for both the forest background scene and the LCM algorithm. In the sky background scene, the proposed algorithm reduces the false alarm rate by 9.09% compared to the LMWIE algorithm. The proposed algorithm can achieve accurate detection of targets while minimizing the introduction of interference information. This is due to the better filtering ability of the proposed

Table 1. Probability of false alarm of three different scenes.

| Algrithom | Ground as background | Forests and buildings as background | Clouds as background |
|---|---|---|---|
| LCM | 0.3750 | 0 | 0.1304 |
| MPCM | 0.1927 | 0.2040 | 0.1972 |
| LMWIE | 0.1304 | 0.04762 | 0.0909 |
| Proposed | 0.1111 | 0 | 0 |

algorithm in different intervals using different contrast measurement methods to filter out interfering objects, as well as the dual-contrast enhancement effect on targets.

## 5. Conclusion

The article proposes a hierarchical local contrast metric-based method for detecting infrared small targets. This method employs different contrast measurement techniques based on the grayscale range, building on traditional small object detection algorithms that rely on human vision. The algorithm not only considers the spatial discontinuity of small targets but also takes into account the unique energy distribution characteristics of low-contrast small target areas, eliminating the impact of bright targets and interference objects on detection results. Experimental results demonstrate that the proposed algorithm effectively reduces false alarm rates while enhancing the signal-to-noise ratio of infrared small target images. The algorithm has advantages in detecting small targets in common ground and sky backgrounds, as well as various complex scenes such as forests. The drawback of the article lies in the high time complexity of the algorithm and the high hardware performance requirements for algorithm implementation. Therefore, future research should focus on improving computational efficiency of the algorithm.

## References

[1] H. Shi, Z. Fang, Y. Wang, L. Chen, An adaptive sample assignment strategy based on feature enhancement for ship detection in SAR images, Remote. Sens. 14 (9) (2022) 2238. doi:10.3390/rs14092238.
[2] H. Shi, C. He, J. Li, L. Chen, Y. Wang, An improved anchor-free sar ship detection algorithm based on brain-inspired attention mechanism, Frontiers in Neuroscience 16. doi:10.3389/fnins.2022.1074706.
[3] Y. Han, H. Liu, Y. Wang, C. Liu, A comprehensive review for typical applications based upon unmanned aerial vehicle platform, IEEE J. Sel. Top. Appl. Earth Obs. Remote. Sens. 15 (2022) 9654–9666. doi:10.1109/JSTARS.2022.3216564.
[4] Y. Han, C. Deng, B. Zhao, D. Tao, State-aware anti-drift object tracking, IEEE Transactions on Image Processing PP (99).
[5] Y. Han, H. Wang, Z. Zhang, Z. Wang, Boundary-aware vehicle tracking upon uav, Electronics Letters.
[6] L. Wu, X. Jin, X. Shi, The development of infrared detection technology, Laser and Infrared.
[7] S. D. Deshpande, H. E. Meng, V. Ronda, P. Chan, Max-mean and max-median filters for detection of small-targets, 1999.
[8] M. F. Seyed, M. M. Reza, N. Mahdi, Flying small target detection in ir images based on adaptive toggle operator, IET Computer Vision 12 (4) (2018) 527–534.
[9] C. Gao, D. Meng, Y. Yang, Y. Wang, X. Zhou, A. G. Hauptmann, Infrared patch-image model for small target detection in a single image, IEEE Transactions on Image Processing 22 (12) (2013) 4996–5009.
[10] J. Zhao, Z. Tang, J. Yang, E. Liu, Infrared small target detection using sparse representation, Journal of systems engineering and electronics 22 (6) (2011) 8.
[11] J. Han, M. Yong, Z. Bo, F. Fan, K. Liang, F. Yu, A robust infrared small target detection algorithm based on human visual system, IEEE Geoscience and Remote Sensing Letters 11 (12) (2014) 2168–2172.
[12] C. Chen, H. Li, Y. Wei, T. Xia, Y. Y. Tang, A local contrast method for small infrared target detection, IEEE Transactions on Geoscience and Remote Sensing 52 (1) (2013) 574–581.
[13] Y. Wei, X. You, H. Li, Multiscale patch-based contrast measure for small infrared target detection, Pattern Recognition 58 (2016) 216–226.
[14] X. Liu, Z. Zuo, A dim small infrared moving target detection algorithm based on improved three-dimensional directional filtering, Springer Berlin Heidelberg.
[15] S. Moradi, P. Moallem, M. F. Sabahi, Fast and robust small infrared target detection using absolute directional mean difference algorithm - sciencedirect, Signal Processing 177.
[16] L. Wu, Y. Ma, F. Fan, M. Wu, J. Huang, A double-neighborhood gradient method for infrared small target detection, IEEE Geoscience and Remote Sensing Letters 18 (8) (2021) 1476–1480. doi:10.1109/LGRS.2020.3003267.